

Synthesis and Characterization of Copper, Nickel and Cobalt Complexes of *N,N'*-Dimethyl-2,11-diaza[3,3](2,6)pyridinophane

Hans-Jörg Krüger

Institut für Anorganische und Angewandte Chemie der Universität Hamburg,
Martin-Luther-King-Platz 6, D-20146 Hamburg, Germany

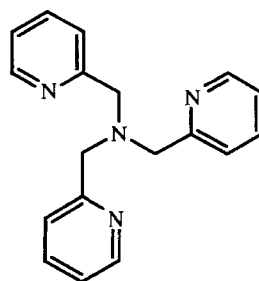
Received August 23, 1994

Key Words: 2,11-Diaza[3,3](2,6)pyridinophane, *N,N'*-dimethyl- / Tetraazamacrocyclic complexes / *cis*-Octahedral coordination geometry

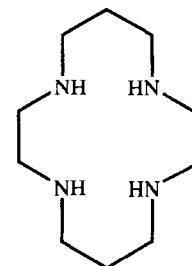
The properties of the tetraazamacrocyclic compound *N,N'*-dimethyl-2,11-diaza[3,3](2,6)pyridinophane ($L-N_4Me_2$) as a ligand for some selected metal chlorides have been examined. The crystal structure of the uncoordinated ligand reveals a *syn* chair-chair conformation. In solution, the ligand displays fluctional behavior. Reaction of $L-N_4Me_2$ with the chlorides of copper(II), nickel(II), and cobalt(II) affords the complexes $[Cu(L-N_4Me_2)Cl_2] \cdot H_2O$ (**3**), $[Ni(L-N_4Me_2)(H_2O)Cl]Cl \cdot H_2O$ (**4**), and $[Co(L-N_4Me_2)Cl_2] \cdot 2 H_2O$ (**5**) in which the ligand adopts a *syn* boat-boat conformation. The crystal

structures of **4** and **5** are presented. Due to the small cavity of the 12-membered ring of the ligand, exclusively distorted *cis*-octahedral coordination geometries are found at the metal sites. A comparison of structural data of several complexes with this ligand shows that the extent of the distortions from ideal octahedral geometry is mainly determined by the $M-N_{py}$ bond strength. The electronic as well as the solution properties of the described complexes have been investigated by electronic absorption spectroscopy, ESR spectroscopy, and electrochemical methods.

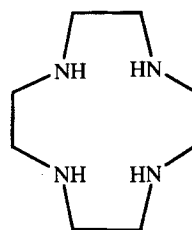
As a part of our research efforts in investigating the effects of structural aspects from a coordinated ligand on the reactivity occurring at the metal site of a complex, we searched for a suitable tetradentate ligand which fulfills several requirements. First, it should contain nitrogenous donor atoms. In addition, the ligand needs to form octahedral complexes with various metal ions where two *cis* coordination sites can be occupied by a wide variety of additional ligands. Further, the ligand should have some functional options for implementation of steric hindrance to avoid formation of dinuclear complexes. To ensure coordination of all four nitrogen atoms at any time, the ligand should also be macrocyclic. Acyclic ligands with four potential donor atoms like tpa^[1] have been shown in some cases to act as tridentate ligands^[2]. In other instances, 14-membered tetraazamacrocyclic rings like cyclam can coordinate to metal ions in the required fashion to leave two *cis* coordination sites at the disposal of additional ligand donors^[3]. However, this *cis*-octahedral geometry occurs only in the presence of bidentate ligands or due to specific synthetic procedures. In the vast majority of complexes, cyclam acts as an equatorial ligand^[4]. Smaller rings, like the 12-membered macrocycle cyclen, usually afford cavities which are too small to allow coordination of the ligand in an equatorial plane^[5,6]. The utilization of cyclen for our purposes was impeded by two considerations. First, cyclen is a very flexible ligand and, although unusual, allows accommodation of square-planar nickel ions^[7]. Further, attachment of sterically demanding substituents to the nitrogen atoms results in the formation of square-pyramidal rather than octahedral complexes^[8,9,10].



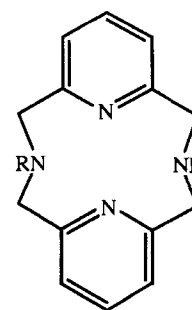
tpa



cyclam



cyclen



R = H: $L-N_4H_2$

R = Me: $L-N_4Me_2$

Therefore, 2,11-diaza[3,3](2,6)pyridinophane ($L-N_4H_2$) was chosen as a starting point for our research. Similar to cyclen, $L-N_4H_2$ consists of a 12-membered macrocyclic ring. However, in contrast to cyclen, considerable steric

rigidity is introduced by the two pyridine rings in $L-N_4H_2$. Because of this, fewer conformers are possible for $L-N_4H_2$, and the cavity is too restricted to allow any equatorial coordination. In addition, pyridine nitrogen atoms form stronger $M-N$ bonds and, together with the macrocyclic chelate effect, this ensures coordination of all nitrogens to the metal ions. With appropriate substituents at the amine nitrogens, sufficient steric hindrance can be achieved to protect the two additional donor atoms from nucleophilic attack without preventing their coordination. Ligand $L-N_4H_2$ and its derivatives have the further advantage that they can be synthesized with relative ease^[11,12].

In this report, the structural aspects of N,N' -dimethyl-2,11-diaza[3,3](2,6)pyridinophane $L-N_4Me_2$ and its dynamic behavior in solution will be discussed with regard to its complexation properties. The capability of this compound to bind to $Cu(II)$ and $Rh(III)$ has been previously demonstrated, but except for the structure determinations the reports lack any further characterization of the complexes^[13,14]. Here, the syntheses of the $Co(II)$, $Ni(II)$, and $Cu(II)$ chloride complexes with this ligand are described. A detailed characterization of the isolated complexes in the solid state as well as in solution, together with a comparison of the structural aspects of the complexes, will provide additional insights into the unique properties of $L-N_4Me_2$ as a ligand.

Results and Discussion

The primary objective of this investigation is the characterization of complexes with the ligand $L-N_4Me_2$ in the solid state and in solution. Although the synthesis of $L-N_4Me_2$ has been previously reported, no detailed study of the structural aspects of this compound has yet been made. Therefore, before addressing the properties of a few selected metal chloride complexes, the results of the structural investigations of the ligand are presented here.

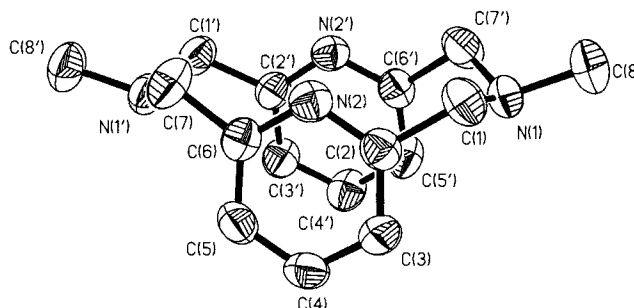
Structural Determination of the Ligand $L-N_4Me_2$

A structural determination was carried out on a single crystal of the free ligand (Figure 1, selected distances and angles in the legend). The molecule, which possesses approximate C_{2v} symmetry, has in its solid state a crystallographically imposed C_2 symmetry. The structure of $L-N_4Me_2$ resembles, in its conformational aspects as well as in its structural parameters, that of the only recently investigated N,N' -di-*tert*-butyl-2,11-diaza[3,3](2,6)pyridinophane^[12].

The 12-membered macrocyclic ring of the uncoordinated ligand exhibits a chair-conformation with both methyl groups on the tertiary amine nitrogens in equatorial positions. This conformation has also been reported to occur in other derivatives of [3.3](2,6)pyridinophanes^[12,15] and [3.3]metacyclophanes^[16]. In these nearly rectangular rings the atoms of the cyclic zig-zag chain can be envisioned as alternating between two layers. In contrast, cyclen is best described as a large square with the ring atoms alternately occupying three layers^[17]. The structural differences be-

tween these 12-membered rings can be attributed to the presence of sp^2 -hybridized atoms in cyclophanes and pyridinophanes.

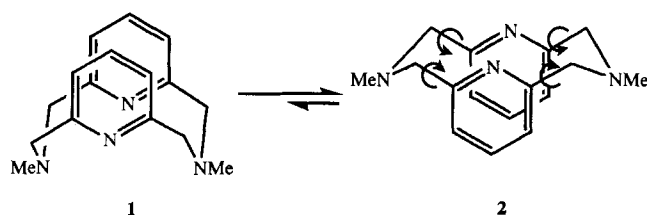
Figure 1. Structure of $L-N_4Me_2$ showing 50-% ellipsoids and the atom numbering scheme. The primed and unprimed atoms are related by a two-fold axis. Selected distances [Å] and angles [°]: $N(1)-C(1)$ 1.467(2), $C(1)-C(2)$ 1.506(2), $N(2)-C(2)$ 1.340(2), $N(2)-C(6)$ 1.334(2), $C(6)-C(7)$ 1.513(2), $C(7)-N(1')$ 1.466(2); $C(1)-N(1)-C(7')$ 113.3(1), $N(1)-C(1)-C(2)$ 112.5(1), $N(2)-C(2)-C(1)$ 116.7(1), $C(2)-N(2)-C(6)$ 118.0(1), $N(2)-C(6)-C(7)$ 116.3(1), $N(1')-C(7)-C(6)$ 113.5(1)



The two pyridine rings of $L-N_4Me_2$ are nearly parallel with an angle of 17.9° included by the two pyridine planes. This *syn* conformation is retained in solution as the 1H -NMR signals at $\delta = 6.75$ and 7.12 for the *meta*- and *para*-pyridyl protons, respectively, demonstrate. Similar conformations are also observed for other [3.3](2,6)pyridinophane derivatives^[15].

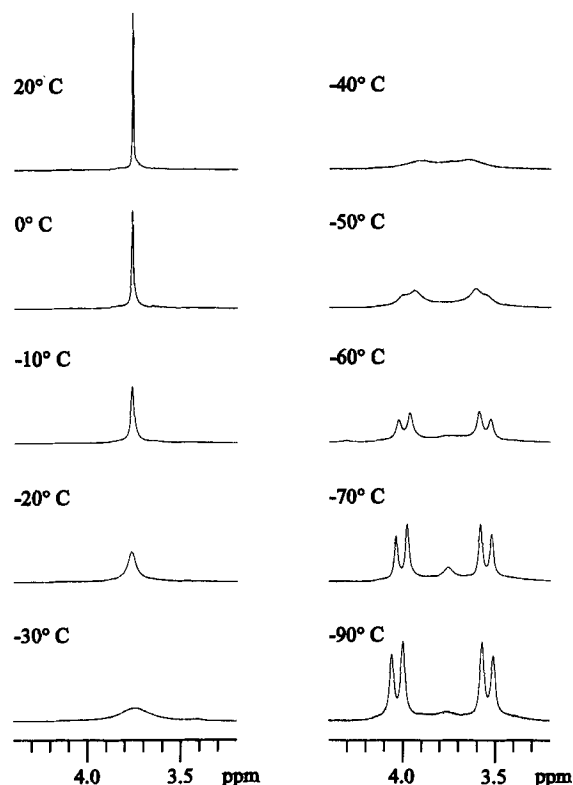
The methylene carbons are displaced from the least-squares pyridine planes by 0.14 and 0.21 Å towards the amine nitrogens. The angles included by the macrocyclic ring atoms at the amine nitrogen and the methylene carbon atoms are slightly larger than expected in unstrained compounds. Apart from these findings, no other structural parameters indicate any obvious strain caused by the macrocyclic nature of ligand $L-N_4Me_2$.

The opposite orientations of the lone pairs on the pyridine and the amine nitrogens are noteworthy. In order to act as a tetradentate ligand, all the lone pairs on the nitrogen atoms are, however, required to point towards a vacant coordination site, and the ligand must be present in a boat-boat conformation as depicted by the conformer **1**. Preliminary force-field calculations^[18] have been carried out to obtain an estimated value for the energy difference between the conformer **2** found in the solid state and the one needed for complexation (**1**). Calculations on the molecule in the gas phase as well as when it is imbedded in a solvent matrix confirm the lowest energy for conformer **2**. Depending on the applied force field, conformer **1** lies energetically 8.5 to 20.5 kJ/mol higher than **2**. This entails that at room temperature some molecules occupy the appropriate conformation for complexation. Further, this estimated energy difference indicates that no major additional strain is introduced into the ligand portion when conformation **1** is adopted during complexation of the metal ion. The expenditure of 20.5 kJ/mol is easily balanced by the energy gain due to formation of four metal-nitrogen bonds.



The dynamic nature of the free ligand has been investigated by means of NMR techniques. In Figure 2, the singlet at room temperature illustrates that the diastereotopic hydrogens at the methylene carbons in $L-N_4Me_2$ easily interconvert. Lowering of the temperature results in the appearance of an AB splitting pattern for the methylenic protons. At a coalescence temperature of about $-35^\circ C$ the conversion rate is about 214 s^{-1} ; from this a free energy of activation ΔG^\ddagger of $47 \pm 2\text{ kJ/mol}$ can be estimated. In minor amounts at $-70^\circ C$ a second, not yet identified conformer can be resolved due to the appearance of additional peaks.

Figure 2. 1H -NMR signals of the methylene protons of $L-N_4Me_2$ in methanol solution at different temperatures

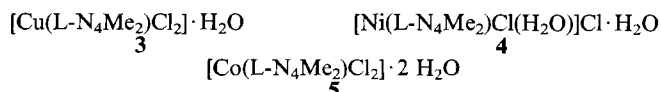


The observance of equivalent methylene hydrogen atoms at room temperature requires an intramolecular process composed of atomic inversions at both amine nitrogens and several rotations around single bonds. Based on a comparison of the free energy of activation with that for the inversion of trimethylamine ($\Delta G^\ddagger = 31.4\text{ kJ/mol}$ at 300 K)^[19], the rate-determining step is attributed to the inversion. Considering the relative ease of this intramolecular conversion, one can assume that the equilibrium between both conformers **1** and **2** will be quite rapidly established since it would only involve rotations around C–C bonds. There-

fore, coordination of the ligand in its boat-boat conformation does not seem to be impeded by thermodynamic or kinetic factors.

Properties of the Complexes in the Solid State

The complexes **3**–**5** were prepared from the corresponding metal(II) chlorides and equivalent amounts of free ligand $L-N_4Me_2$ in 96% ethanol solutions. As solids, all compounds are air-stable. In solution, however, compound **5** exhibits slight oxygen sensitivity. The magnetic moments μ_B of 1.90, 3.19, and 5.16 B.M. for the compounds **3**, **4** and **5**, respectively, are consistent with their formulation as octahedral complexes^[10,20].



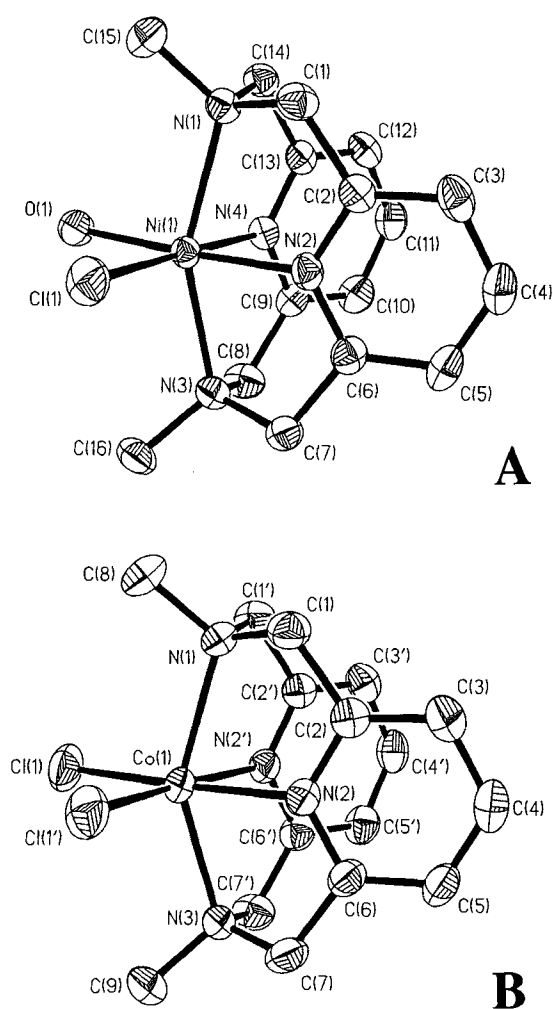
Structures of $[Ni(L-N_4Me_2)Cl(H_2O)]Cl \cdot H_2O$ (**4**) and $[Co(L-N_4Me_2)Cl_2] \cdot 2 H_2O$ (**5**)

Structural determinations were undertaken for all three complexes. Since structural data on the copper complex **3** ($R = 3.58\%$) agree with those obtained by Fronczek et al.^[13] within experimental errors, our data will not be further presented here except for comparisons of bond distances and angles. Perspective views of the complexes **4** and **5** are shown in Figure 3.

In all complexes, the ligand $L-N_4Me_2$ provides four nitrogen donor atoms for coordination. Due to its small ring size, the ligand is folded along the $N_{amine}-N_{amine}$ axis upon complexation and, therefore, exclusively *cis*-octahedral geometries are found in complexes with this ligand. Formation of a planar nickel(II) complex, even if in a rather distorted geometry as observed with other 12-membered macrocyclic ligands like cyclen^[7], is prohibited by the enforced rigidity due to the two pyridine rings in $L-N_4Me_2$. Experiments with $L-N_4Me_2$, utilizing specific reaction conditions applied to cyclen derivatives^[7], have not shown any evidence of equatorial coordination of the ligand. The axial coordination sites are occupied by the two amine nitrogen atoms; and the pyridine nitrogen atoms coordinate two *cis* positions in the equatorial plane. Thereby two *cis*-equatorial sites – from here on referred to as *cis* coordination sites – are left open for two additional ligand donors (e.g. chloride and water). It is worthwhile to point out that the methyl substituents on the amine nitrogen atoms are positioned above and below the two additional ligand donors, hence providing some steric protection to the two *cis*-coordinating ligands without impeding their coordination^[12]. This feature has been shown to become quite prominent in reactivity studies of other metal complexes with this ligand.

Similar to the structurally related complex $[Ni(cyclen-Me_2)Br(H_2O)]^+[1,6b]$, the two *cis* coordination sites in the nickel complex are occupied by a chloride and a water molecule. Some of the more prominent structural features like the folding of the ligand moiety along the axis formed by the tertiary amines and the location of the methyl groups above and below the *cis* coordination sites are also preva-

Figure 3. Structure of $[\text{Ni}(\text{L}-\text{N}_4\text{Me}_2)\text{Cl}(\text{H}_2\text{O})]^+$ (A) and $[\text{Co}(\text{L}-\text{N}_4\text{Me}_2)\text{Cl}_2]$ (B) showing 50-% ellipsoids and the atom numbering schemes. A: Selected distances [Å] and angles [°]: Ni(1)–N(1) 2.195(3), Ni(1)–N(2) 2.019(4), Ni(1)–N(3) 2.203(3), Ni(1)–N(4) 2.023(4), Ni(1)–Cl(1) 2.383(1), Ni(1)–O(1) 2.128(4); N(1)–Ni(1)–N(2) 80.5(2), N(1)–Ni(1)–N(3) 154.1(1), N(1)–Ni(1)–N(4) 80.2(2), N(1)–Ni(1)–Cl(1) 99.2(1), N(1)–Ni(1)–O(1) 97.3(2), N(2)–Ni(1)–N(3) 80.2(2), N(2)–Ni(1)–N(4) 82.6(1), N(2)–Ni(1)–Cl(1) 93.2(1), N(2)–Ni(1)–O(1) 174.2(2), N(3)–Ni(1)–N(4) 80.3(2), N(3)–Ni(1)–Cl(1) 99.0(1), N(3)–Ni(1)–O(1) 100.2(2), N(4)–Ni(1)–Cl(1) 175.7(1), N(4)–Ni(1)–O(1) 91.8(2), Cl(1)–Ni(1)–O(1) 92.5(1). – B: The primed and unprimed atoms are related by a mirror plane. Selected distances [Å] and angles [°]: Co(1)–N(1) 2.257(3), Co(1)–N(2) 2.107(2), Co(1)–N(3) 2.244(3), Co(1)–Cl(1) 2.401(1); N(1)–Co(1)–N(2) 77.58(7), N(1)–Co(1)–N(3) 148.21(9), N(1)–Co(1)–Cl(1) 100.24(4), N(2)–Co(1)–N(3) 79.56(10), N(2)–Co(1)–N(3) 78.12(7), N(2)–Co(1)–Cl(1) 170.86(5), N(2)–Co(1)–Cl(1') 91.31(5), N(3)–Co(1)–Cl(1) 100.50(5), Cl(1)–Co(1)–Cl(1') 97.82(4)



lent here. In both complexes the Ni–N distances to the axial tertiary amine nitrogen atoms are larger than those to the equatorial pyridine or secondary amine nitrogen atoms. In $[\text{Ni}(\text{L}-\text{N}_4\text{Me}_2)\text{Cl}(\text{H}_2\text{O})]^+$, the Ni–N_{py} distances average to 2.021 Å while the mean Ni–N_{amine} distance measures 2.199 Å. This increase of the bond distances by 0.178 Å is more prominent than the corresponding changes in $[\text{Ni}(\text{cyclenMe}_2)\text{Br}(\text{H}_2\text{O})]^+$. The Ni–N_{py} lengths fall into the

range of distances observed for molecules where a pyridyl group is part of a multidentate ligand with five-membered chelate rings^[21]. Although not the longest, the average Ni–N_{amine} distance of 2.199 Å is considerably longer than the mean Ni–N distance of 2.088 Å found in molecules with tertiary amine units as part of a multidentate ligand system with five-membered chelate ring sizes^[21]. The Ni–O and Ni–Cl bond lengths of 2.131 and 2.383 Å, respectively, are consistent with those obtained in structural determinations of other nickel complexes^[21].

The nickel atom and all four equatorial donor atoms lie within 0.013 Å in a plane. While all angles in the equatorial plane approach octahedral standards, a severe deviation in the angle N_{amine}–Ni–N_{amine} from 180 to 154.2° is observed. A similar angle has also been measured in $[\text{Ni}(\text{cyclenMe}_2)\text{Br}(\text{H}_2\text{O})]^+$. As a result of the steric constraints imposed by the two essentially planar pyridine rings, the metal ion does not lie on the intersecting line of both pyridine planes but 0.549 and 0.596 Å above either plane. Both pyridine planes include an angle of 49.0°. A comparison of bond distances and angles of the free and the bound ligand does not reveal any obvious strain exerted on the ligand by coordination. However, the average NCCN intraannular torsion angle of 113.7° in the uncoordinated ligand decreases to the remarkably low value of 35.7° upon complexation.

In contrast to the nickel complex, both *cis* coordination sites are occupied by chloride ions in $[\text{Co}(\text{L}-\text{N}_4\text{Me}_2)\text{Cl}_2]$. Here, the complex exhibits a crystallographically imposed C_s symmetry. The Co–N_{py} distance of 2.107 Å is approximately the same as the mean six-coordinate Co(II)–N bond length when the pyridine moiety is part of a multidentate ligand with five-membered chelate rings^[21]. As in the nickel complex, the Co–N_{amine} bonds are quite large with an average length of 2.251 Å. This distance is not the largest, but still considerably above the mean Co–N distance of 2.151 Å found in octahedral Co(II) complexes where the tertiary amine is an analogous part of a multidentate ligand^[21]. The Co–Cl bond length of 2.401 Å compares well with those of other six-coordinate cobaltous chlorides^[21].

Compared with the nickel complex, a more pronounced deviation from octahedral geometry is observed as manifested by the smaller N_{amine}–Co–N_{amine} and N_{py}–Co–N_{py} angles of 148.2 and 79.6°, respectively. The cobalt ion is found within 0.006 Å in the plane of the equatorial donor atoms. The deviation of the cobalt ion from the least-squares pyridine plane is, with 0.572 Å, comparable to the previously discussed deviations in the nickel complex. Here, in the cobalt complex, the angle included by the pyridine planes measures only 47.0°.

Comparison of Structural Parameters of Divalent Metal Chloride Complexes with L-N₄Me₂

Table 1 contains averaged bond distances and angles from various divalent metal chlorides coordinated to the ligand L-N₄Me₂. Where applicable, all the metal ions occupy the high-spin state. The following order of decreasing M–N_{py} bond distances has been established: Mn(II) >

Table 1. Comparative structural data of metal(II) chloride complexes with the ligand L-N₄Me₂^[a]

	[Mn(L-N ₄ Me ₂)Cl ₂] ^[b]	[Fe(L-N ₄ Me ₂)Cl ₂] ^[b]	[Co(L-N ₄ Me ₂)Cl ₂] ^[c]	[Ni(L-N ₄ Me ₂)Cl(H ₂ O)] ^[c]	[Cu(L-N ₄ Me ₂)Cl ₂] ^[b,d]	[Zn(L-N ₄ Me ₂)Cl ₂] ^[b]
M-N _{py} (Å)	2.269	2.177	2.107	2.023	2.070	2.173
M-N _{amine} (Å)	2.374	2.298	2.251	2.198	2.353	2.304
N _{amine} -M-N _{amine} (°)	138.8	142.9	148.2	154.2	147.9	144.0
N _{py} -M-N _{py} (°)	73.7	76.0	79.6	82.5	79.0	76.8
angle between pyridinal planes (°)	42.2	46.0	47.0	49.0	50.2	45.1
d (Å) ^[e]	0.59	0.55	0.57	0.57	0.50	0.58
N _{amine} ...N _{amine} (Å)	4.44	4.36	4.33	4.29	4.52	4.38
Shannon radius (Å) ^[f]	0.97	0.92	0.885	0.83	0.87	0.88

^[a] Mean values of distances and angles. — ^[b] H.-J. Krüger, unpublished results. — ^[c] This work. — ^[d] Data from ref.^[13]. — ^[e] Metal ion displacement from the least-squares planes of the pyridine rings. — ^[f] R. D. Shannon, *Acta Crystallogr., Sect. A*, **1976**, 32, 751.

Fe(II) \approx Zn(II) > Co(II) > Cu(II) > Ni(II). This order corresponds approximately to that one found for the effective ionic radii of divalent high-spin metal ions in octahedral geometries, which is determined by the increase of the effective nuclear charge on the metal ion as well as by the number of electrons in the σ -antibonding e_g^* orbitals. However, π bonding interactions between the metal ion and the pyridine nitrogen atoms acting as π acceptors have to be invoked to provide adequate explanation for the greater shortening of the M-N_{py} bonds, going from Mn(II) to Ni(II), than that predicted by the effective ionic radii.

In comparison with the M-N_{amine} bonds, the interactions between the metal ion and the pyridine nitrogen atoms are stronger, and their influence is much more pronounced in defining the structural aspects of the binding of the ligand to the metal. With divalent metal chloride complexes, it is found that the metal ion is drawn further into the cavity of the macrocyclic ring by stronger M-N_{py} interactions. However, the extremely small cavity still causes the metal ion to protrude, generating N_{amine}-M-N_{amine} angles of much less than 180°. From this discussion it can be concluded that a smaller N_{amine}-M-N_{amine} as well as a smaller N_{py}-M-N_{py} angle are expected to be found with decreasing M-N_{py} bond length. While the pyridine planes of the uncoordinated ligand are nearly coplanar and include an angle of only 17.9°, the orientations of both planes readjust to allow better overlap of the nitrogen lone pairs with the d orbitals on the metal ion upon coordination. However, the macrocyclic restraints limit the reorientation of the planes, thus, in the case of divalent metal ions, allowing only angles of 42 to 50° between the pyridine planes to occur. In general, the angle is diminished when the metal ions are accommodated at a shorter M-N_{py} distance. Due to restricted adjustment of the ligand upon coordination, the metal ions are displaced by about 0.50 to 0.59 Å out of the pyridine plane.

With the exception of the copper complex, M-N_{amine} bond lengths follow the same order as the M-N_{py} bonds. The M-N_{amine} bond length is in part determined by the M-N_{py} distance and by the size of the amine substituents^[12], but also to some extent by expansion of the cavity of the ligand as revealed by the increase of the N_{amine}...N_{amine} distance from 4.29 Å (Ni) to 4.44 Å (Mn)

and 4.54 Å (Cu). The limited conformational freedom of the ligand permits a steric rearrangement of the CH₂-NMe-CH₂ chains with the likely purpose of enhancing interactions between the amine nitrogen atoms and the metal ion jutting out of the cavity to various extents. In the copper complex, this conformational freedom also allows the elongation of the axial bonds attributed to the Jahn-Teller distortion.

Properties of the Complexes in Solution

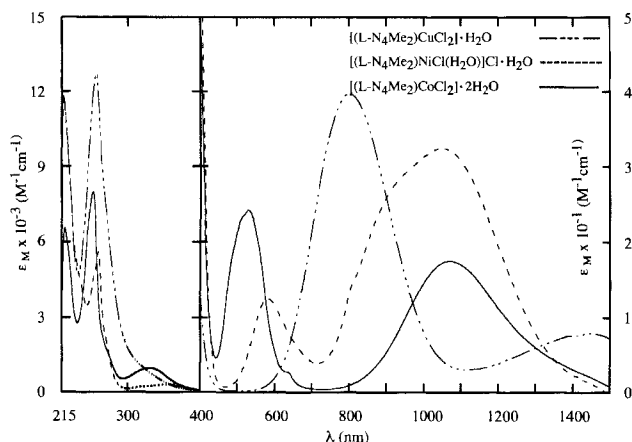
Of all the transition metal chloride complexes isolated so far with the ligand L-N₄Me₂, the corresponding nickel compound is unique since it crystallizes as a cationic complex where at one coordination site the chloro ligand is replaced by a water molecule. This finding led to the investigation of the nature of the complexes in solutions. The results of the conductivity measurements performed on 1 mM solutions of the complexes in MeOH, MeCN, and water are listed in Table 2. These measurements indicate that in MeOH the compounds behave as one-to-one electrolytes whereas in water both chloride ions are dissociated^[9a,10]. In contrast to the one-to-one electrolytic behavior of a 1 mM solution of **4** in acetonitrile, solutions of compounds **3** and **5** in the same solvent display only partial dissociation of one of the coordinated chloride ions. The absorption spectra of all three complexes in methanol solution are presented in Figure 4, and the electronic absorption maxima together with their molar extinction coefficients and their tentative assignments are listed in Table 2.

By ESR spectroscopy the ground-state electron configuration of the copper complex was determined to be $...(d_{x^2-y^2})^1$ ^[22]. In Figure 5, the ESR spectrum of [Cu(L-N₄Me₂)Cl₂] in an ethanol glass at 77 K consists of an axial signal with $g_{\perp} = 2.077$ and $g_{\parallel} = 2.312$ ^[23]. The rather small value for the parallel Cu hyperfine coupling constant, A_{\parallel}^{Cu} , of $150 \cdot 10^{-4} \text{ cm}^{-1}$, together with the relatively high value for g_{\parallel} , are indicative of a copper complex in a distorted octahedral environment with mostly nitrogen donor atoms^[22,24]. No hyperfine coupling to any of the nitrogen atoms of the ligand could be resolved. The observed ESR as well as the electronic absorption spectra^[25] of the dissolved complex are most consistent with a tetragonally distorted octahedral geometry in which the axial bonds are elongated

Table 2. Conductivity and electronic absorption data for the compounds 3, 4, 5, and $\text{L-N}_4\text{Me}_2$ in various media

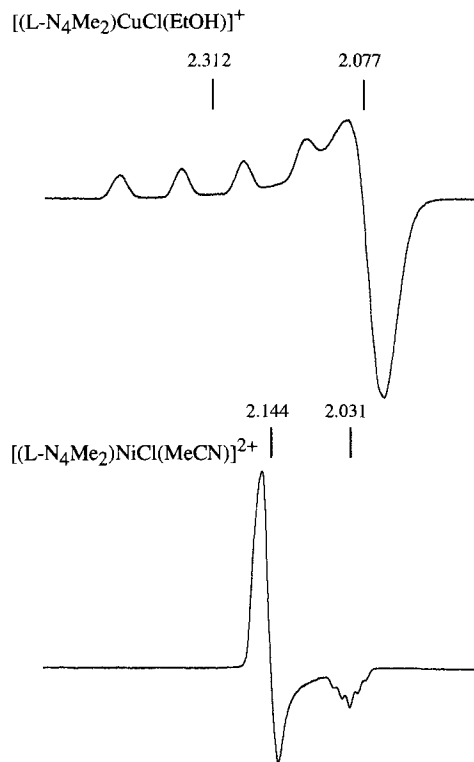
Compound	Conductance ^[a] , Λ , $\Omega^{-1} \text{ cm mole}^{-1}$		
	H_2O	MeOH	MeCN
$[\text{Cu}(\text{L-N}_4\text{Me}_2)\text{Cl}_2] \cdot \text{H}_2\text{O}$	221	81.0	14.6
$[\text{Ni}(\text{L-N}_4\text{Me}_2)\text{Cl}(\text{H}_2\text{O})]\text{Cl} \cdot \text{H}_2\text{O}$	211	85.4	74.6
$[\text{Co}(\text{L-N}_4\text{Me}_2)\text{Cl}_2] \cdot 2\text{H}_2\text{O}$	220	86.5	36.4
Electronic Absorption Maxima λ_{max} (ϵ_{M} , assignments ^[b])			
$[\text{Cu}(\text{L-N}_4\text{Me}_2)\text{Cl}_2] \cdot \text{H}_2\text{O}$ in MeOH	217 (11800), 260 (12700), 799 (39.8, d_{xz} , d_{yz} , $d_{xy} \rightarrow d_{x^2-y^2}$) and 1450 (7.94, $d_{z^2} \rightarrow d_{x^2-y^2}$) nm		
solid state	854 and 1505 nm		
$[\text{Ni}(\text{L-N}_4\text{Me}_2)\text{Cl}(\text{H}_2\text{O})]\text{Cl} \cdot \text{H}_2\text{O}$ in MeOH	217 (11700), 263 (5590), 357 (310, CT or $^3\text{A}_{2g} \rightarrow ^3\text{T}_{1g}(\text{P})$), 583 (12.5, $^3\text{A}_{2g} \rightarrow ^3\text{T}_{1g}$), 930 (sh, 28.0, $^3\text{A}_{2g} \rightarrow ^1\text{E}_g$) and 1050 (32.4, $^3\text{A}_{2g} \rightarrow ^3\text{T}_{2g}$) nm		
solid state	358, 583 and 953 nm		
$[\text{Co}(\text{L-N}_4\text{Me}_2)\text{Cl}_2] \cdot 2\text{H}_2\text{O}$ in MeOH	218 (6530), 256 (7950), 333 (967), 530 (24.2, $^4\text{T}_{1g} \rightarrow ^4\text{T}_{1g}(\text{P})$) and 1069 (17.5, $^4\text{T}_{1g} \rightarrow ^4\text{T}_{2g}$) nm		
solid state	359, 499, 526, 557 and 1139 nm		
$\text{L-N}_4\text{Me}_2$ in MeOH	ca. 200 and 260 nm		

[a] At 25 °C in 1 mM solutions. – [b] Tentative, based on ref.^[24] assuming a pseudo-octahedral geometry with the $\text{N}_{\text{amine}}-\text{N}_{\text{amine}}$ axis orientated along the z direction.

Figure 4. Electronic absorption spectra of $[\text{Cu}(\text{L-N}_4\text{Me}_2)\text{Cl}_2] \cdot \text{H}_2\text{O}$ (3), $[\text{Ni}(\text{L-N}_4\text{Me}_2)\text{Cl}(\text{H}_2\text{O})]\text{Cl} \cdot \text{H}_2\text{O}$ (4), and $[\text{Co}(\text{L-N}_4\text{Me}_2)\text{Cl}_2] \cdot 2\text{H}_2\text{O}$ (5) in methanol solution

and are incompatible with either a square-pyramidal^[9a,22c,26,27] or a trigonal-bipyramidal geometry^[22c,25,27]. This result is corroborated by the crystal structure of the complex. The solid-state spectrum shows rather similar absorption bands. The comparison with the solution spectrum strongly supports the conclusion that octahedral geometry is preserved upon dissolution of the complex and that the coordination site of the dissociated chloride ion is now occupied by a solvent molecule. The blue-shift of about 55 nm for the ligand field bands is also understandable considering that the coordinated MeOH exerts a slightly stronger ligand field than a chloride ion. In frozen acetonitrile solution, where hardly any replacement of the chloro ligand by the solvent occurs, the ESR spectrum of the com-

plex (not shown) exhibits a slightly different axial signal with $g_{\parallel} = 2.067$, $g_{\perp} = 2.299$, and $A_{\parallel}^{\text{Cu}} = 140 \cdot 10^{-4} \text{ cm}^{-1}$. The differences in g and A_{\parallel} values agree with the coordination of a solvent molecule to the copper ion in methanol solutions.

Figure 5. X-Band ESR spectra of $[\text{Cu}(\text{L-N}_4\text{Me}_2)\text{Cl}_2] \cdot \text{H}_2\text{O}$ (3) in ethanol and electrochemically generated $[\text{Ni}(\text{L-N}_4\text{Me}_2)\text{Cl}(\text{MeCN})]^{2+}$ in acetonitrile glasses at 77 K; apparent g values are indicated

The decisive preference of the ligand $\text{L-N}_4\text{Me}_2$ for octahedral rather than trigonal-bipyramidal or square-pyramidal geometries is remarkable since tetradentate ligands with nitrogen donors usually form five- rather than six-coordinate $\text{Cu}(\text{II})$ complexes^[9,26,27].

The UV-Vis spectrum of $[\text{Ni}(\text{L-N}_4\text{Me}_2)\text{Cl}(\text{H}_2\text{O})]^+$ in methanol solution, especially the higher intensity for the lowest energy absorption band than that for the second transition, agrees with a *cis*-octahedral geometry^[6b,8,25,28]. The rather small differences between the solid-state and the solution spectra clearly confirm the octahedral geometry of the dissolved complex and its identity as an one-to-one electrolyte.

The electronic absorption spectrum of $[\text{Co}(\text{L-N}_4\text{Me}_2)\text{Cl}_2]$ in methanol is consistent with that of a six-coordinate high-spin $\text{Co}(\text{II})$ ion^[25]. High-spin trigonal-bipyramidal and square-pyramidal geometries can be excluded on the basis of intensities and positions of the absorption bands^[10,25]. From the general similarities of electronic absorption spectra of the solid and the dissolved cobalt complex, and considering the results of the conductivity experiments, it is concluded that the overall octahedral geometry of the complex is also preserved in solution. As in the previously discussed copper complex, the observed blue-shift of the d-d

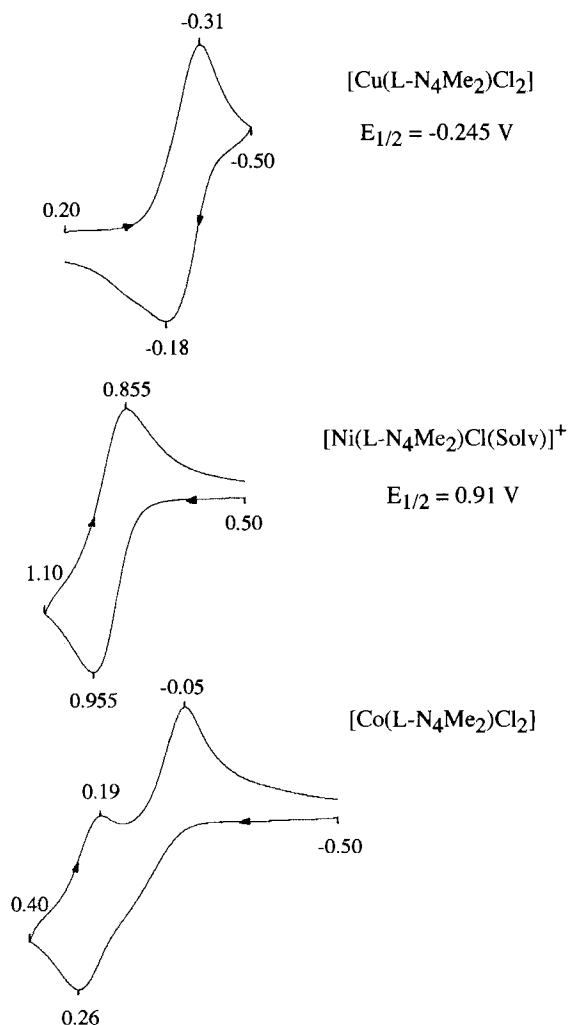
bands upon dissolving the complex in methanol supports the conclusion regarding the replacement of one coordinated chloride ion by a solvent molecule.

The redox properties of the complexes in acetonitrile solutions have been investigated by cyclic voltammetry as presented in Figure 6. The copper chloride complex displays a reduction potential at -0.245 V vs. SCE. From the line shape of the oxidation peak, the electron transfer reaction must be considered to some extent as irreversible. Since Cu(I) complexes normally do not entertain octahedral geometries, the irreversibility may be caused by dissociation of bound chloride ions from the reduced complex. Dissolving equivalent amounts of Cu(II) perchlorate and ligand $L-N_4Me_2$ in acetonitrile results in the formation of a blue complex whose ESR spectrum with $g_{\parallel} = 2.071$, $g_{\perp} = 2.284$, and $A_{\text{Cu}}^{\text{Cu}} = 164 \cdot 10^{-4} \text{ cm}^{-1}$ is consistent with the formation of the complex as $[Cu(L-N_4Me_2)(MeCN)_2]^{2+}$. In contrast to the electrochemical behavior of the copper chloride complex, this complex exhibits a quasi-reversible Cu(II/I) redox potential at $+0.11$ V with a peak potential difference ΔE_p of 80 mV. This result emphasizes that the irreversibility of the redox reaction of the copper chloride complex should be attributed to the loss of chloro ligands in the reduced species rather than to any dissociation of the ligand $L-N_4Me_2$. No evidence for demetallation of the reduced copper complexes is observed. In accordance with copper(II) cyclen complexes^[26] the here described copper(II) complex with a 12-membered macrocyclic ring is easier to reduce than those with 13 to 16-membered rings^[29].

In acetonitrile solution, $[Ni(L-N_4Me_2)Cl(H_2O)]^+$ can be electrochemically oxidized at 0.91 V. The redox reaction displays quasi-reversibility since $\Delta E_p = 100$ mV at a scan rate v of 50 mV/s, $i_{p,a}/i_{p,c} \approx 1$, and $i_p/v^{1/2}$ is independent of the scan rate. Coulometric oxidation of the complex at an applied potential of 1.10 V produces a dark violet solution. After oxidation of the complex by exactly one electron, the observed constant, albeit small, residual current as well as the recovery of only 80–90% of the reduced complex upon re-reduction, demonstrate some decomposition of the oxidized complex. The ESR spectrum of the immediate oxidation product, depicted in Figure 5, consists of a rhombic signal with $g_{zz} = 2.031$, $g_{yy} = 2.144$, and $g_{xx} = 2.163$. The $g_{av} = 2.113$ and the substantial g tensor anisotropy clearly indicate a metal-centered oxidation. Due to interactions of the electron spin with the nuclear spins ($I_N = 1$) of the two axial amine nitrogen atoms, the g_{zz} component of the signal exhibits a superhyperfine quintet with $A_{zz}^N = 18.0$ G. From $g_{zz} \approx 2.0$ and $g_{xx}, g_{yy} > g_{zz}$, together with the observed superhyperfine splitting, an electron configuration $\dots(d_{z^2})^1$ is inferred. The comparatively low $g_{xx,yy}$ and A_{zz}^N values which are normally higher than 2.17 and 20 G, respectively, for nickel(III) tetraazamacrocyclic complexes with the same electronic ground state^[30], are also consistent with the evident elongation of the axial bonds in this complex.

A mixture of equivalent amounts of ligand and nickel(II) perchlorate in acetonitrile affords an octahedral complex, which shows a Ni(III/II) redox potential at 1.79 V ($\Delta E_p = 80$ mV). This value is about 400 mV higher than that ob-

Figure 6. Cyclic voltammograms (50 mV/s) of $[Cu(L-N_4Me_2)Cl_2] \cdot H_2O$ (3), $[Ni(L-N_4Me_2)Cl(H_2O)]Cl \cdot H_2O$ (4), and $[Co(L-N_4Me_2)Cl_2] \cdot 2 H_2O$ (5) at a Pt-foil electrode in acetonitrile solutions at 25°C; peak potentials and half-wave potentials vs. SCE are indicated



tained for the corresponding nickel complex with cyclen as ligand^[30b]. In addition, the different redox potential for $[Ni(L-N_4Me_2)(MeCN)_2]^{2+}$ also confirms that 4 is a monocationic species in acetonitrile solutions.

The cobalt chloride complex in acetonitrile solution displays a more complicated cyclic voltammogram. The complex is oxidized at a potential of 0.26 V. In addition to the reduction at 0.19 V, a second reduction occurs at -0.05 V, presumably since some chemical reaction involving the chloride ions follows the initial electron transfer. A cyclic voltammogram of a 1:1 mixture of Co(II) perchlorate and the ligand in acetonitrile reveals only one quasi-reversible oxidation at 0.39 V with peak potentials separated by 70 mV at a scan rate of 50 mV/s.

Conclusions

The following are the principal results and conclusions of this investigation: (1) The ligand $L-N_4Me_2$ acts as a suitable tetradentate ligand for a variety of metal ions. It displays a

decisive tendency to form *cis*-octahedral complexes. Structural aspects of the coordination of the ligand to a metal ion are for the most part determined by the size of the metal ion and the σ - and π -bonding interactions between the metal and the pyridine nitrogen atoms in the equatorial plane. As a result, the axial M–N_{amine} bonds are quite elongated. The length of these bonds is a salient feature in dictating the electronic ground states in Jahn-Teller theorem-affected complexes with d⁹ and low-spin d⁷ metal ions.

(2) In methanol, the constitution of all the discussed metal chloride complexes is best described by the formula [M(L-N₄Me₂)Cl(MeOH)]⁺. This shows that the *cis* coordination sites are easily accessible to other ligands. Therefore, the ligand can be conceived as specifically protecting four coordination sites at an octahedral metal ion from any nucleophilic reagent and, hence, permitting the occurrence of distinctive reactions at defined *cis* coordination sites.

(3) The ligand exhibits some stability towards oxidative reactions as illustrated in the electrochemical oxidation of the nickel complex **4**. This property should not be depreciated especially when the ligand can be employed in metal complex-supported oxidations of organic substrates.

With its remarkable coordination properties, L-N₄Me₂ provides access to new complexes with interesting structural aspects and reactivities in the classic area of coordination chemistry. The reaction chemistry, which takes place at these *cis* coordination sites, is currently under intensive investigation and will be the subject of forthcoming publications.

The support of this research by a grant from the *Deutsche Forschungsgemeinschaft* and the financial assistance by the *University of Hamburg* are greatly appreciated.

Experimental

¹H NMR: Varian Gemini 200 MHz. The accuracy of the temperature measurement of the sample was determined to be $\pm 8^\circ\text{C}$. – UV-Vis: Varian Cary 5 E. The spectra of solid samples were obtained in Nujol mulls by using the diffuse-transmittance technique^[31]. – IR: Perkin-Elmer 1720 FT-IR. – ESR: Bruker ER200tt, interfaced to a computer. The magnetic field was constantly recorded by a Lake Shore 450 Gaussmeter. The spectra were recorded at 77 K on samples in an ethanol glass or in an acetonitrile glass containing 0.2 M (NBu₄)ClO₄. The Ni(III) sample was electrolytically prepared and immediately frozen in liquid nitrogen. – Electrochemistry: PAR Model 270 Research Electrochemistry Software-controlled Potentiostat/Galvanostat Model 273A with the electrochemical cell placed in a glove box. Electrochemical experiments were performed on 1 mM acetonitrile solutions containing 0.2 M (Bu₄N)ClO₄ as supporting electrolyte; a higher than normal electrolyte concentration was applied to minimize solution resistance. All potentials were measured vs. a SCE reference electrode at 25°C. The potentials were not corrected for junction potentials. A Pt-foil electrode was employed as the working electrode. Acetonitrile was dried with CaH₂ and freshly distilled prior to use. Under this condition the potential for the Fc/Fc⁺ couple was 0.39 V. Coulometric experiments were performed by using a Pt gauze electrode. – Magnetic susceptibilities: Johnson Matthey Magnetic Susceptibility Balance. The magnetic susceptibility of the ligand L-N₄Me₂ was measured to be $-1.758 \cdot 10^{-4}$ emu/mol. Susceptibilities of chlo-

rides and water molecules were taken from a standard source^[32]. – Conductivity experiments: WTW LF 521 with a calibrated electrode at 25°C.

Preparation of Compounds: The ligand *N,N'*-dimethyl-2,11-diaza[3,3](2,6)pyridinophane (L-N₄Me₂) was synthesized according to published procedures with some slight modifications^[11]. All other chemicals were purchased and used without further purification.

General Procedure for Preparing the Metal Complexes: An ethanolic solution (5 ml) of 1.0 mmol of metal chloride was added dropwise to a hot solution of 268 mg of the ligand L-N₄Me₂ (1.0 mmol) in 5 ml of 96% ethanol. Upon heating, the volume of the solution was reduced by half. Slow cooling of the solution and subsequent standing for 2 d at ambient temp. afforded analytically pure, crystalline products. The yield can be enhanced by a further reduction of the volume of the mother liquid and additional storage of it.

[Cu(L-N₄Me₂)Cl₂] · H₂O (**3**): From 170 mg of CuCl₂ · 2 H₂O (1.0 mmol) a total yield of 348 mg (73%) of light green crystalline product was achieved. – C₁₆H₂₂Cl₂CuN₄O (420.8): calcd. C 45.66, H 5.27, N 13.31; found C 45.71, H 5.36, N 13.41. – IR (KBr): $\tilde{\nu}$ = 3452, 3400, 1597, 1581, 1458, 1443, 1031, 1014, 880, 811, 794, 759 cm⁻¹ (strong bands only). – Magnetic moment μ_B : 1.90 B.M.

[Ni(L-N₄Me₂)(H₂O)Cl]Cl · H₂O (**4**): From 238 mg of NiCl₂ · 6 H₂O (1.0 mmol) a total amount of 410 mg of crystalline blue product (94%) was obtained. – C₁₆H₂₄Cl₂N₂NiO₂ (434.0): calcd. C 44.28, H 5.57, N 12.91; found C 44.44, H 5.71, N 12.99. – IR (KBr): $\tilde{\nu}$ = 3514, 3446, 3218, 1605, 1581, 1475, 1446, 1382, 1008, 817, 805 cm⁻¹ (strong bands only). – Magnetic moment μ_B : 3.19 B.M.

[Co(L-N₄Me₂)Cl₂] · 2 H₂O (**5**): From 130 mg of CoCl₂ (1.0 mmol) under nitrogen a total yield of 291 mg of violet crystalline product (67%) was achieved. – C₁₆H₂₄Cl₂CoN₄O₂ (434.2): calcd. C 44.25, H 5.57, N 12.90; found C 44.32, H 5.52, N 12.80. – IR

Table 3. Crystal data, intensity collection and refinement parameters for L-N₄Me₂, [Ni(L-N₄Me₂)Cl(H₂O)]Cl · H₂O (**4**), and [Co(L-N₄Me₂)Cl₂] · 2 H₂O (**5**)

Data	L-N ₄ Me ₂	4	5
formula	C ₁₆ H ₂₀ N ₄	C ₁₆ H ₂₄ Cl ₂ N ₄ NiO ₂	C ₁₆ H ₂₄ Cl ₂ CoN ₄ O ₂
molecular weight, g mol ⁻¹	268.36	434.00	434.22
crystal dimensions, mm	0.25 x 0.4 x 0.7	0.45 x 0.7 x 0.8	0.45 x 0.6 x 0.9
crystal system	orthorhombic	orthorhombic	orthorhombic
space group	<i>Fdd2</i> (No. 43)	<i>P2₁2₁2₁</i> (No. 19)	<i>Pnma</i> (No. 62)
Z	8	4	4
a, Å	19.117(3)	8.918(2)	15.098(3)
b, Å	24.461(4)	14.200(3)	14.145(2)
c, Å	6.352(1)	14.849(3)	8.989(2)
V, Å ³	2970.3(8)	1880.4(7)	1919.7(6)
d _{calc} , g/cm ³	1.20	1.53	1.50
diffractometer	Enraf-Nonius CAD4	Syntex P2 ₁	Syntex P2 ₁
temperature, K	293	293	293
λ , Å	1.54178 (Cu-K α)	0.71073 (Mo-K α)	0.71073 (Mo-K α)
μ , cm ⁻¹	5.77	13.33	11.89
<i>F</i> (000)	1152	904	900
scan method	ω -2 θ	θ -2 θ	θ -2 θ
2 θ limits, deg	11.7 \leq 2 θ \leq 152.4	5.4 \leq 2 θ \leq 55.2	5.4 \leq 2 θ \leq 55.1
unique reflections	1422	4316	2301
reflections with $F_o > 4 \sigma(F_o)$	1411	4015	1892
number of variables (restraints)	96	238	132
Goof on χ^2 [a]	1.050	1.064	1.120
<i>R</i> (wR^2), % [a, b, c]	3.10 (8.36)	6.80 (17.8)	4.00 (11.5)

[a] For all reflections with $F_o > 4\sigma(F_o)$. – [b] $R = \sum \|F_o\| - \|F_c\| / \sum \|F_o\|$. – [c] $wR^2 = \{\sum [w(F_o^2 - F_c^2)] / \sum [w(F_o^2)]\}^{1/2}$.

(KBr): $\tilde{\nu} = 3514, 3443, 3209, 1605, 1580, 1474, 1446, 1023, 1011, 811 \text{ cm}^{-1}$ (strong bands only). — Magnetic moment μ_B : 5.16 B.M.

X-Ray Structure Determinations of $L\text{-N}_4\text{Me}_2$, $[\text{Ni}(L\text{-N}_4\text{Me}_2)\text{Cl}(\text{H}_2\text{O})]\text{Cl} \cdot \text{H}_2\text{O}$, and $[\text{Co}(L\text{-N}_4\text{Me}_2)\text{Cl}_2] \cdot 2 \text{H}_2\text{O}$: Suitable single crystals of the free ligand, of **4** and **5** were obtained by recrystallization from hexane and 96% ethanol, respectively. For data collection the crystals were glued onto glass-fibers. Cell parameters for all crystals and experimental details on the data collections and the structure refinements are contained in Table 3^[33]. The structures were solved by direct methods and refined by full-matrix least squares on F^2 , utilizing the programs SHELXS-86 and SHELXL-93. All non-hydrogen atoms were anisotropically refined. The hydrogen atoms of the bound water molecule in compound **4** and the water molecules in compound **5** were located by Fourier difference maps, and their locations were isotropically refined. The hydrogen atoms of the uncoordinated water molecule in **4** could not be located and were therefore not included in the calculations. All residual hydrogen atoms were placed in ideal positions and isotropically refined. The largest difference peaks (holes) were 0.162 (−0.117), 1.230 (−1.161), and 0.302 (−1.013) $e/\text{\AA}^3$ for compounds $L\text{-N}_4\text{Me}_2$, **4** and **5**, respectively.

- [1] Abbreviations: tpa = tris(2-pyridylmethyl)amine; cyclam = 1,4,8,11-tetraazacyclotetradecane; cyclen = 1,4,7,10-tetraazacyclododecane; $L\text{-N}_4\text{H}_2 = 2,11\text{-diaza}[3,3](2,6)\text{pyridinophane}$; $L\text{-N}_4\text{Me}_2 = N,N'\text{-dimethyl-2,11-diaza}[3,3](2,6)\text{pyridinophane}$; cyclen $\text{Me}_2 = 1,7\text{-dimethyl-1,4,7,10-tetraazacyclododecane}$.
- [2] R. R. Jacobson, Z. Tyeklar, A. Farooq, K. D. Karlin, S. Liu, J. Zubieta, *J. Am. Chem. Soc.* **1988**, *110*, 3690–3692.
- [3] ^{3a)} E. K. Barefield, A. Bianchi, E. J. Billo, P. J. Connolly, P. Paoletti, J. S. Summers, D. G. Van Derveer, *Inorg. Chem.* **1986**, *25*, 4197–4202. — ^{3b)} L. P. Battaglia, A. Bianchi, A. B. Corradi, E. Garcia-Espana, M. Micheloni, M. Julve, *Inorg. Chem.* **1988**, *27*, 4174–4179. — ^{3c)} D. A. House, V. McKee, *Inorg. Chem.* **1984**, *23*, 4237. — ^{3d)} K. Beveridge, O. Heyd, A. D. Kirk, *Acta Crystallogr., Sect. C*, **1993**, *49*, 1063–1066. — ^{3e)} T. F. Lai, C. K. Poon, *Inorg. Chem.* **1976**, *15*, 1562–1566. — ^{3f)} K. J. Brewer, M. Calvin, R. S. Lumpkin, J. W. Otvos, L. O. Spreer, *Inorg. Chem.* **1989**, *28*, 4446–4451.
- [4] U. Henrick, P. H. Tasher, L. F. Lindoy, *Prog. Inorg. Chem.* **1985**, *33*, 1–58.
- [5] ^{5a)} Y. Iitaka, M. Shina, E. Kimura, *Inorg. Chem.* **1974**, *13*, 2886–2891. — ^{5b)} J. H. Loehlin, E. B. Fischer, *Acta Crystallogr., Sect. B*, **1976**, *32*, 3063–3066. — ^{5c)} S. Tsuboyama, K. Tsuboyama, T. Sakurai, J. Uzawa, *Inorg. Nucl. Chem. Lett.* **1980**, *16*, 267–270. — ^{5d)} N. Matsumoto, A. Hirano, T. Hara, A. Ohyoshi, *J. Chem. Soc., Dalton Trans.* **1983**, 2405–2410. — ^{5e)} J. Giusti, S. Chimichi, M. Ciampolini, M. Sabat, D. Masi, *Inorg. Chim. Acta* **1984**, *88*, 51–54. — ^{5f)} R. G. Swisher, G. A. Brown, R. C. Smierciak, E. L. Blinn, *Inorg. Chem.* **1981**, *20*, 3947–3951.
- [6] ^{6a)} R. Smierciak, J. Passariello, E. L. Blinn, *Inorg. Chem.* **1977**, *16*, 2646–2648. — ^{6b)} M. Ciampolini, M. Micheloni, N. Nardi, P. Paoletti, P. Dapporto, F. Zanobini, *J. Chem. Soc., Dalton Trans.* **1984**, 1357–1362.
- [7] ^{7a)} L. Fabbri, *Inorg. Chem.* **1977**, *16*, 2667–2668. — ^{7b)} W. H. Plassman, R. G. Swisher, E. L. Blinn, *Inorg. Chem.* **1980**, *19*, 1101–1103. — ^{7c)} J. H. Coates, D. A. Hadi, S. F. Lincoln, H. W. Dodgen, J. P. Hunt, *Inorg. Chem.* **1981**, *20*, 707–711. — ^{7d)} J. H. Coates, D. M. M. A. Hadi, T. W. Hambley, S. F. Lincoln, J. R. Rodgers, *Cryst. Struct. Commun.* **1982**, *11*, 815–820.
- [8] G. A. Kalligeros, E. L. Blinn, *Inorg. Chem.* **1972**, *11*, 1145–1148.
- [9] ^{9a)} M. C. Styka, R. C. Smierciak, E. L. Blinn, R. E. DeSimone, J. V. Passariello, *Inorg. Chem.* **1978**, *17*, 82–86. — ^{9b)} R. E. DeSimone, E. L. Blinn, K. F. Mucker, *Inorg. Nucl. Chem. Lett.* **1980**, *16*, 23–26. — ^{9c)} T. Sakurai, K. Kobayashi, A. Hasegawa, S. Tsuboyama, K. Tsuboyama, *Acta Crystallogr., Sect. B*, **1982**, *38*, 107–111. — ^{9d)} K. Kobayashi, T. Sakurai, A. Hasegawa, S. Tsuboyama, K. Tsuboyama, *Acta Crystallogr., Sect. B*, **1982**, *38*, 1154–1158. — ^{9e)} T. Sakurai, K. Kobayashi, H. Masuda, S. Tsuboyama, K. Tsuboyama, *Acta Crystallogr., Sect. B*, **1983**, *39*, 334–337.
- [10] C. M. Sarther, E. L. Blinn, *Inorg. Chem.* **1976**, *15*, 3083–3087.
- [11] ^{11a)} F. Bottino, M. Di Grazia, P. Finocchiaro, F. R. Fronczek, A. Mamo, S. Pappalardo, *J. Org. Chem.* **1988**, *53*, 3521–3529. — ^{11b)} B. Alpha, E. Anklam, R. Deschenaux, J.-M. Lehn, M. Pietraskiewicz, *Helv. Chim. Acta* **1988**, *71*, 1042–1052.
- [12] C.-M. Che, Z.-Y. Li, K.-Y. Wong, C.-K. Poon, T. C. W. Mak, S.-M. Peng, *Polyhedron* **1994**, *13*, 771–776.
- [13] F. R. Fronczek, A. Mamo, S. Pappalardo, *Inorg. Chem.* **1989**, *28*, 1419–1422.
- [14] H. Sakaba, C. Kabuto, H. Horino, M. Arai, *Bull. Chem. Soc. Jpn.* **1990**, *63*, 1822–1824.
- [15] G. R. Newkome, S. Pappalardo, F. R. Fronczek, *J. Am. Chem. Soc.* **1983**, *105*, 5152–5153.
- [16] ^{16a)} M. F. Semmelhack, J. J. Harrison, D. C. Young, A. Gutierrez, S. Rafii, J. Clardy, *J. Am. Chem. Soc.* **1985**, *107*, 7508–7514. — ^{16b)} W. Anker, G. W. Bushnell, R. H. Mitchell, *Can. J. Chem.* **1979**, *57*, 3080–3087.
- [17] J. H. Reibenspies, *Acta Crystallogr., Sect. C*, **1992**, *48*, 1717–1718.
- [18] P. Krüger, H.-J. Krüger, unpublished results: Calculations were carried out with the program package MacroModel V 3.0 (W. C. Still, F. Mohamadi, N. G. J. Richards, W. C. Guida, M. Lipton, R. Liskamp, G. Chang, T. Hendrickson, S. DeGust, W. Hasel, Dept of Chemistry, Columbia University, New York, NY 10027) by using the internal force fields MM2, MM3, and Amber with the solvent option of dichloromethane.
- [19] A. Zschunke, *Molekülstruktur*, Spektrum Akademischer Verlag, Heidelberg, **1993**, p. 113.
- [20] ^{20a)} L. Sacconi, F. Mani, A. Bencini in *Comprehensive Coordination Chemistry*, vol. 5 (Eds.: G. Wilkinson, R. D. Gillard, J. A. McCleverty), Pergamon Press, Oxford, **1987**, chapter 50. — ^{20b)} B. J. Hathaway, ref.^[20a], chapter 53.
- [21] ^{21a)} Cambridge Structural Database 5.07, April 1994. — ^{21b)} A. G. Orpen, L. Brammer, F. H. Allen, O. Kennard, D. G. Watson, R. Taylor, *J. Chem. Soc., Dalton Trans.* **1989**, S1–S83.
- [22] ^{22a)} B. R. McGarvey, *Transition Met. Chem.* **1966**, *3*, 89–201. — ^{22b)} A. H. Maki, N. Edelstein, A. Davison, R. H. Holm, *J. Am. Chem. Soc.* **1964**, *86*, 4580–4587. — ^{22c)} B. J. Hathaway, D. E. Billing, *Coord. Chem. Rev.* **1970**, *5*, 143–207.
- [23] For a molecule with C_{2v} symmetry a rhombic ESR signal is expected. However, if the energy differences between the d_{xz} and the d_{yz} orbitals (assuming a pseudo-octahedral geometry with the N_{amine} – N_{amine} axis orientated along the z direction) are small, then the rhombicity might be obscured by the rather large linewidth of the signal.
- [24] K. Miyoshi, H. Tanaka, E. Kimura, S. Tsuboyama, S. Murata, H. Shimizu, K. Ishizu, *Inorg. Chim. Acta* **1983**, *78*, 23–30.
- [25] A. B. P. Lever, *Inorganic Electronic Spectroscopy*, 2nd ed., Elsevier Science Publishers B.V., Amsterdam, **1984**.
- [26] R. L. Webb, M. L. Mino, E. L. Blinn, A. A. Pinkerton, *Inorg. Chem.* **1993**, *32*, 1396–1402.
- [27] K. D. Karlin, J. C. Hayes, S. Juan, J. P. Hutchinson, J. Zubieta, *Inorg. Chem.* **1982**, *21*, 4106–4108.
- [28] ^{28a)} C. K. Jørgensen, *Acta Chem. Scand.* **1956**, *10*, 887–910. — ^{28b)} S. A. Rasmussen, *Acta Scand. Chem.* **1959**, *13*, 2009–2022. — ^{28c)} J. D. Vitiello, E. J. Billo, *Inorg. Chem.* **1980**, *19*, 3477–3481.
- [29] ^{29a)} P. Zanello, R. Seeber, A. Cinquantini, G.-A. Mazzocchin, L. Fabbri, *J. Chem. Soc., Dalton Trans.* **1982**, 893. — ^{29b)} L. Fabbri, A. Poggi, P. Zanello, *J. Chem. Soc., Dalton Trans.* **1983**, 2191.
- [30] ^{30a)} F. V. Lovecchio, E. S. Gore, D. H. Busch, *J. Am. Chem. Soc.* **1974**, *96*, 3109–3118. — ^{30b)} A. Bencini, L. Fabbri, A. Poggi, *Inorg. Chem.* **1981**, *20*, 2544–2549.
- [31] R. H. Lee, E. Griswald, J. Kleinberg, *Inorg. Chem.* **1964**, *3*, 1279–1283.
- [32] F. E. Mabbs, D. J. Machin, *Magnetism and Transition Metal Complexes*, Chapman and Hall, London, **1973**.
- [33] Further details to these structure determinations can be obtained from the Fachinformationszentrum Karlsruhe, Gesellschaft für wissenschaftlich-technische Information mbH, D-76344 Eggenstein-Leopoldshafen, by indicating the deposition number CSD-401414 ($L\text{-N}_4\text{Me}_2$), CSD-401415 (**4**), or CSD-401416 (**5**), the author's name and the publication reference.

[337/94]